Transient States of Matter during Short Pulse Laser Ablation

K. Sokolowski-Tinten, J. Bialkowski, A. Cavalleri, and D. von der Linde
Institut für Laser- und Plasmaphysik, Universität-GHS-Essen, D-45117 Essen, Germany

A. Oparin and J. Meyer-ter-Vehn
Max-Planck-Institut für Quantenoptik, Hans-Kopfermann-Strasse 1, D-85748 Garching, Germany

S. I. Anisimov
Landau Institute of Theoretical Physics, Russian Academy of Science, Institutskii prospekt 12, Chernogolovka, Russia
(Received 20 March 1998)

Short pulse laser ablation of semiconductors and metals is studied by means of ultrafast time-resolved microscopy. The characteristic stages of the conversion of solid material into hot fluid matter undergoing ablation are identified. Initially metallic material transforms during the expansion into a transparent state with a high index of refraction. [S0031-9007(98)06502-8]

PACS numbers: 79.20.Ds

Removal of material from the surface of a solid after laser irradiation is commonly called laser ablation. This process plays an important role for structuring and processing of materials in many areas of technology [1]. Laser ablation is also of great interest from a basic physics point of view. To be removed from the surface a change of the fundamental state of aggregation of the material must take place. Transitions between aggregation states are often accompanied by other changes of the physical and chemical character of the material, e.g., a change of chemical bonding or a metal-insulator transition [2].

The particular nature of the ablation process may be strongly dependent on the type of material and on laser intensity, wavelength, duration, and number of pulses. Recent experimental work has indicated that the use of pico- or femtosecond laser pulses may offer some advantages over pulses of longer duration [3]. A distinctive feature of short pulse ablation is that laser-material interaction is separated in time from the actual removal of material. Ultrashort pulses also provide a way of creating much higher energy densities in condensed matter. However, the fundamental physical mechanisms of laser ablation have not been clearly identified as yet, and conflicting views can be found in the literature [4].

We have studied laser ablation in metals and semiconductors using single, well-defined short laser pulses. We are able to identify the fundamental physical mechanisms of short pulse laser ablation for energies relatively close to the threshold, before the onset of plasma formation. In brief, after thermalization of the laser energy the material is left in a fluid state of approximately solid density and high temperature. The hot fluid is subsequently carried away by hydrodynamic flow. The expanding material exhibits interesting thermodynamic, hydrodynamic, and optical properties which will be described in this paper.

In our experiments the structural changes of the material are recorded using time-resolved optical microscopy [5]. A pump pulse excites a surface layer and initiates the ablation. The excited surface area is illuminated with a weak, time-delayed probe pulse and observed with a high resolution optical microscope. Picture frames with a spatial resolution of a few micrometers and a temporal resolution of about 10^{-13} s (determined by the duration of the probe pulses) can be recorded at arbitrary instants after the excitation pulse. Thus, all stages of the evolution of the surface morphology can be recorded. In most cases we used laser pulses of 120 fs duration at a wavelength of 620 nm, both for pump and probe.

Examples of characteristic stages of single pulse laser ablation of Si are shown in Fig. 1. These pictures represent time-resolved optical micrographs of the surface viewed in normal direction. The pump pulses were incident from the left at an angle of about 45 degrees. In the upper left corner (0.2 ps) the pump pulse has swept about halfway across the surface. The large increase of

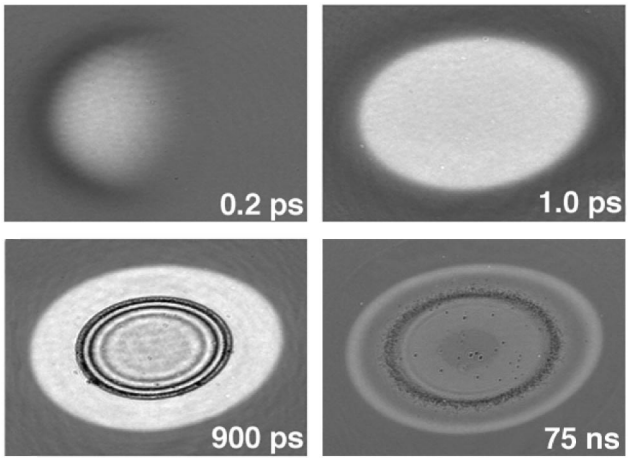

FIG. 1. Surface of a Si wafer after irradiation with a 120 fs laser pulse of 0.47 J/cm^2. Frame size: 220 × 300 μm. Exposure time: 120 fs.

 0031-9007/98/81(1)/224(4)$15.00

the optical reflectivity (bright area) is due to the electron-hole plasma excited by the pump pulse [6]. The very bright, oval-shaped area at slightly later time (1 ps) represents liquid metallic Si (top right). Melting is brought about in less than a picosecond [7] by very strong electronic excitation of the semiconductor [8]. At a much later time (900 ps) a system of distinct dark rings appears in the center of the molten area. The final picture at 75 ns of the resolidified Si surface shows a bright ring at the periphery and a dark ring inside. It can be shown that these features represent, respectively, amorphous Si [9] and the boundary of the ablated area.

The striking feature in Fig. 1 is the system of dark rings observed at about 1 ns. It is the purpose of this paper to show that these rings represent a distinct signature of the ablation process and reveal useful information about the physical mechanisms.

At the outset it may be useful to point out two important general observations: (i) The surface area covered by the dark rings coincides precisely with the ablated surface area. The measured threshold energy [10] for the onset of the ring pattern is identical with the threshold energy of ablation, which can be determined independently from measurements of the size of final ablated area [11]. (ii) We have observed similar phenomena in a wide variety of materials (Si, GaAs, Au, Ti, Al, Hg, Mg). Thus, it appears that the formation of dark rings and laser ablation are closely related and that the underlying physics is of rather general nature.

Figure 2 illustrates these two points by examples of time-resolved micrographs of Ti, Au, Al (metal films on a glass substrate), and bulk Si. The data demonstrate that in all these materials a system of dark rings has developed after a few nanoseconds. Comparison of the final surface morphology of the Al film (bottom, left) with the corresponding time-resolved pictures shows that a thin dark line is left at the circumference of the dark ring area. An independently measured interference micrograph of the same surface area is superimposed on the final morphology for comparison. Note the shift of the interference fringes across the thin line. This shift represents clear evidence that the thin line feature marks the boundary of the ablated area. Measurements of the ablation depth in other materials gave similar results. Thus, we have shown that the surface area covered by the rings represents the ablated area. In the particular case of Fig. 2 the ablated Al layer was approximately 50 nm near the boundary, and somewhat larger in the center. The bottom picture on the right is the spatial profile of the optical reflectivity of the Si example. These data demonstrate the high contrast of the dark rings.

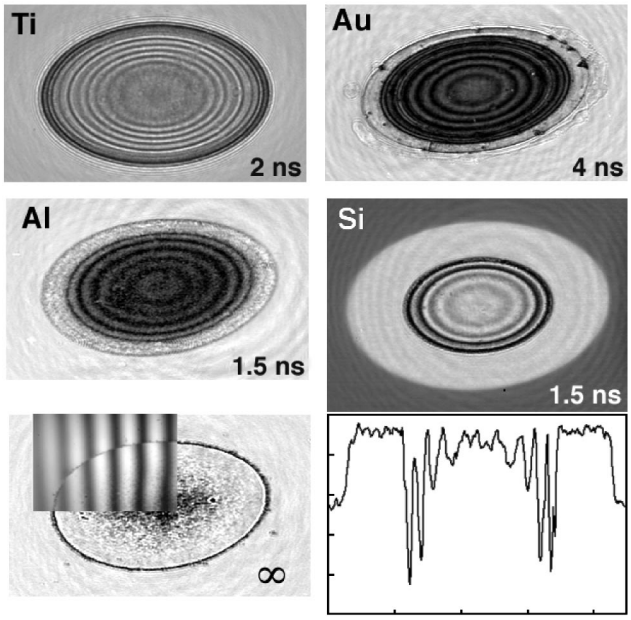

FIG. 2. Top and center row: ring patterns on Ti, Au, Al, and Si. Bottom left: final surface structure of the Al film. Inset: interferogram. Bottom right: reflectivity profile for Si.

Let us now discuss the origin of the dark rings. Diffraction effects due to apertures of the imaging systems could be ruled out by a careful analysis of the spatial frequency spectrum. An actual transient surface structure of molten material could also be excluded, because the feature sizes are dependent on the observation wavelength. In fact, by changing the wavelength of the probe pulses it can be clearly shown that the observed ring features represent high contrast *optical interference patterns* (Newton rings). If the dark rings are interpreted as Newton rings one can immediately determine the optical thickness of the layer between the interfering interfaces. By measuring the changes of the interference patterns as a function of time the relative velocity of the interfering fronts is obtained. If our data are processed correspondingly, we obtain velocities up to about 1000 m/s (Si), depending on the pump pulse energy.

Two basic requirements must be satisfied to explain the observed interference patterns and the high contrast in terms of an expanding layer of ablating material: (1) The ablation process must lead to the formation of a pair of optically flat, sharp interfaces. In particular, the optical density must drop sharply across the interfaces over a distance much smaller than the wavelength; (2) the ablating material must be optically transparent and possess a large index of refraction. To produce the measured fringe contrast in Si, a refractive index $n > 2$ and an absorption coefficient $k < 0.1$ are required.

In the following we show that the observed phenomena follow directly from the changes of the physical properties of initially strongly heated, pressurized matter during free expansion into vacuum. To be specific, we consider the case of Al. Figure 3 shows pressure versus density from tabulated equation-of-state (EOS) data [12]. Let us pursue the path of the material during heating, cooling, and expansion. The thermalization of the laser energy takes

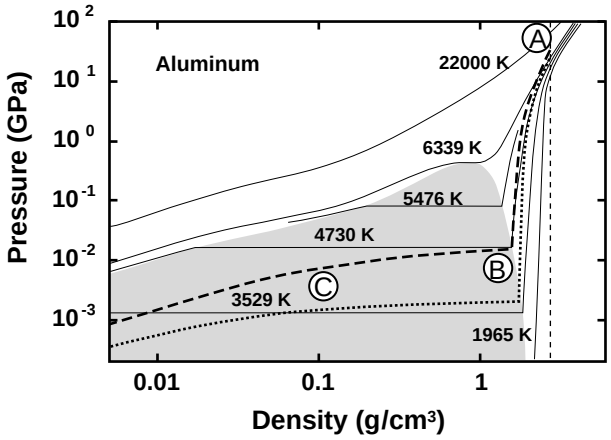

FIG. 3. Pressure vs density from EOS data of Al. Thin lines: isotherms. Gray area: two-phase regime. Thin dashed vertical line: solid density. Dashed and dotted curves: isentropes for initial temperatures of 7000 and 5000 K, respectively.

about 1 ps [13]. This time is too short for significant expansion to occur. Thus, the starting point is solid density material with an initial temperature determined by the amount of deposited energy. We estimate 5000 to 10 000 K near the ablation threshold. The pressure corresponds to several tens of GPa. The initial conditions are indicated by marker (A) in Fig. 3.

The subsequent evolution of the material may be considered as an isentropic expansion into vacuum. The dashed and the dotted lines in Fig. 3 show two isentropes of Al corresponding to initial temperatures of 7000 and 5000 K, respectively. The isentropes cross the binodal boundary of the two-phase regime (gray area) in the neighborhood of marker (B). Nucleation of gas bubbles sets in, and a heterogeneous phase of liquid and gas develops. There is the interesting possibility that strongly superheated conditions occur and that the material is pushed into the spinodal regime [14], where homogeneous matter is thermodynamically unstable [15].

Leaving the possibility of spinodal decomposition as an open question, it can, nevertheless, be concluded that the further evolution of the system is governed by the properties of a heterogeneous liquid-gas mixture. Concerning the dynamics of hydrodynamic expansion, the most significant change of properties in the two-phase regime is a drastic *decrease of the velocity of sound*, $c^2_{\text{sound}} = (\partial p/\partial \rho)_S$ [16]. This is quite apparent from the change of slope of the isentrope at the boundary of the two-phase regime. The regime of low sound velocity is indicated by marker (C).

The change of sound speed is of great significance here. The initial phase of the expansion can be described by a simple one dimensional self-similar rarefaction wave [16]. It follows from Eqs. 92.5 and 92.6 of [16] that, when the decrease of the sound speed is taken into account, the part of the rarefaction wave traveling towards vacuum (tail) develops a sharp front satisfying condition (1). The flow velocity at the vacuum boundary is approximately given by $u \approx c_0 \ln(\rho_1/\rho_0)$, where ρ_0 and ρ_1 are, respectively, the solid density and the liquid density near the binodal boundary [marker (B)]. Detailed computer simulations of the hydrodynamic expansion corroborate this conclusion.

A schematic representation of the early stage of the ablation process is given in Fig. 4. The top panel shows the situation just after energy relaxation, before significant expansion has occurred. The two areas in different shades of gray represent a layer of material of thickness d in above-threshold condition, corresponding to marker (A) in the EOS diagram, and subthreshold material, which will not undergo ablation. The dashed curve in the center panel indicates the profile of the rarefaction wave. The head of the wave travels towards the inside with the sound velocity c_0 of the unperturbed material. The area in light gray represents two-phase material [marker (C)]. As explained above, there is a sharp drop of the density towards vacuum. Thus, the tail of the wave forms a steep moving front, the first density discontinuity.

A second density discontinuity develops after $t_0 = d/c_0$, when the head of the rarefaction wave reaches the boundary of the subthreshold, nonablating material. Now the self-similar character of the rarefaction process is lost. The subsequent evolution can be qualitatively described by regarding the boundary as a rigid wall where the flow velocity vanishes. The reflection of the rarefaction wave produces a drop of the density at the boundary, the second density discontinuity.

The layer thickness d can be estimated from the measured ablation depth, typically 50 to 100 nm. A characteristic value of the sound velocity is 2500 m/s. Thus, the time for the formation of a pair of interfaces is estimated to be $t_0 \approx 20$–40 ps.

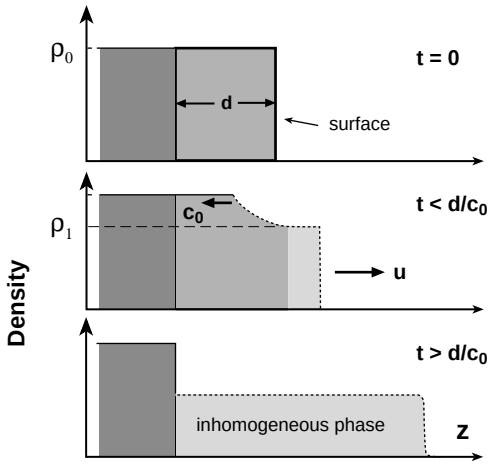

FIG. 4. Dark gray: nonablating material. Gray: expanding homogeneous fluid. Dotted line: rarefaction wave. Light gray: heterogeneous phase gas/liquid. ρ_0: solid density. ρ_1: liquid density.

The situation for $t > t_0$ can be characterized as follows (bottom of Fig. 4): Two sharp interfaces exist which confine a layer of expanding material. After the density in this layer has dropped below ρ_1, the entire ablating material consists of an inhomogeneous mixture of two phases with low average density.

After having explained the formation of the two interfaces, we briefly discuss the optical properties of the confined layer. Refractive indices calculated from a Clausius-Mossotti model of the gaseous phase using tabulated values of the atomic polarizabilities are too low to account for the observed interference phenomena. This is further indication that the ablating material is not a homogeneous gas phase. Concerning the optical properties of a two-component medium a number of models are available [17]. However, for a detailed analysis the nature of the mixed phase must be known, e.g., the structure of the clusters forming the high density component. Unfortunately, this information is not available at the present time. We have used the simple Maxwell-Garnett formula [18] which describes the optical properties of spherical particles immersed in some dielectric medium, provided that the particle sizes are much smaller than the wavelength. Using the optical constants of the metallic liquid for the spheres the corresponding Maxwell-Garnett medium would become transparent upon expansion and exhibit an effective refractive index of about two when the metal droplets fill one-half of the available volume. Thus, even a very crude model of the optical properties of the two-phase medium is capable of qualitatively accounting for the basic experimental observation that the originally metallic ablating material turns into a transparent, highly refractive medium.

In summary, our experiments have revealed the detailed sequence of events in short pulse laser ablation of semiconductors and metals. Ablation can be generally characterized as a rapid thermal process. We have identified the fundamental thermodynamic and hydrodynamic processes underlying laser ablation relatively close to the threshold, before the onset of plasma formation. Our interpretation does not apply to higher peak intensities and laser ablation of insulating materials where optical breakdown and plasma formation play a dominant role [19,3].

More work is required to clarify the optical properties of the heterogeneous phase and the character of the ablation threshold. We believe that the threshold behavior may result from the very strong increase of the nucleation rate with temperature.

Interesting future research includes the possibility of spinodal decomposition, the properties of materials near the critical point, and the possibility of observing metal-insulator transitions.

A. C. gratefully acknowledges support from the European Community through Human Capital and Mobility.

[1] See, e.g., M. von Allmen and A. Blatter, *Laser-Beam Interactions with Matter*, in Springer Series in Material Science, Vol. 2 (Springer, Berlin, 1995), 2nd ed.

[2] Ya. B. Zel'dovich and L. D. Landau, Zh. Eksp. Teor. Fiz. **14**, 32 (1944); F. Hensel, J. Phys. Condens. Matter **2**, 33 (1990).

[3] X. Liu, D. Du, and G. Mourou, IEEE J. Quantum. Electron. **33**, 1706 (1997); B. C. Stuart, M. D. Veit, S. Herman, A. M. Rubenchik, B. W. Shore, and M. D. Perry, Phys. Rev. B **53**, 1749 (1996); W. Kautek, J. Krüger, M. Lenzner, S. Sartania, Ch. Spielmann, and F. Krausz, Appl. Phys. Lett. **69**, 3146 (1996); S. Nolte, C. Momma, H. Jacobs, A. Tünnermann, B. N. Chichkov, B. Wellegehausen, and H. Welling, J. Opt. Soc. Am. B **14**, 2716 (1997).

[4] A. Miotello and R. Kelly, Appl. Phys. Lett. **67**, 3535 (1995).

[5] M. C. Downer, R. L. Fork, and C. V. Shank, J. Opt. Soc. Am. B **4**, 595 (1985).

[6] C. V. Shank, R. Yen, and C. Hirlimann, Phys. Rev. Lett. **50**, 454 (1983).

[7] K. Sokolowski-Tinten, J. Bialkowski, and D. von der Linde, Phys. Rev. B **51**, 14 186 (1995).

[8] P. Stampfli and K. H. Bennemann, Phys. Rev. B **49**, 7299 (1994).

[9] P. L. Liu, R. Yen, N. Bloembergen, and R. T. Hodgson, Appl. Phys. Lett. **34**, 864 (1979).

[10] J. M. Liu, Opt. Lett. **7**, 196 (1982).

[11] The measured ablation thresholds for p-polarized light at $\approx 45°$ are 0.3 J/cm^2 and 0.54 J/cm^2 for Si and Al, respectively.

[12] A. V. Bushman, I. V. Lomonosov, and V. E. Fortov, *Equations of State of Metals at High Energy Densities* (Institute of Chemical Physics, Russian Academy of Sciences, Chernogolovka, 1992) (in Russian).

[13] N. Bloembergen, in *Beam-Solid Interactions and Phase Transformations, 1985*, edited by H. Kurz, G. L. Olson, and J. M. Poate, MRS Symposia Proceedings No. 51 (Materials Research Society, Pittsburgh, 1986), p. 3.

[14] V. P. Skripov and A. V. Skripov, Sov. Phys. Usp. **22**, 389 (1979).

[15] L. D. Landau and E. M. Lifshits, *Course of Theoretical Physics V: Statistical Physics* (Pergamon Press, Oxford, 1978).

[16] L. D. Landau and E. M. Lifshits, *Course of Theoretical Physics VI: Fluid Mechanics* (Pergamon Press, Oxford, 1982).

[17] C. F. Bohren and D. R. Huffman, *Absorption and Scattering of Light by Small Particles* (Wiley Interscience, New York, 1983).

[18] J. C. Maxwell Garnett, Philos. Trans. R. Soc. London A **203**, 385 (1904).

[19] D. von der Linde and H. Schüler, J. Opt. Soc. Am. B **13**, 216 (1996).